Supporting Information for

Constructing an AIE Diphenylquinoxaline-Based Luminescent Europium-Organic Framework for Multiple Substances Sensing

Siji Xu,[a] Gui Xiong,[a] Xiang-Yu Zhang,[a] Kun Huang,[a*] Da-Bin Qin,[a*] Bin Zhao[ab]

[a] Key Laboratory of Chemical Synthesis and Pollution Control of Sichuan Province, School of Chemistry and Chemical Engineering, China West Normal University, Nanchong 637002, P. R. China.

[b] Department of Chemistry, Key Laboratory of Advanced Energy Material Chemistry, Nankai University, Tianjin 300071, P. R. China.

[*]*Corresponding authors, e-mails: hkun2017@cwnu.edu.cn; qdbkyl@cwnu.edu.cn*

Contents

Table S1 Some Ln-MOFs based sensors.

MOFs	Analyte	Medium	K_{sv}/M^{-1}	LOD	Refs
DPQ-Eu	***Fe^{3+}/ Hg^{2+}/ $Cr_2O_7^{2-}$/ CN^-***	***H_2O***	***1.31×10^5/ 1.41×10^5/ 1.71×10^5/ 1.02×10^6***	***25.99 nM/ 39.70 nM/ 9.88 nM/ 8.19 nM***	***This work***
$[Tb(Hmcd)(H_2O)(DMF)_2]_n$	Fe^{3+}/ $Cr_2O_7^{2-}$/ CrO_4^{2-}	DMF	7252.88/ 27328.375/-	5×10^{-6} M/ 1.32×10^{-6} M/ 3.88×10^{-5} M	*S1*
$[Tb_4(L)_6(H_2O)_8]$	Fe^{3+}/ $Cr_2O_7^{2-}$/ CrO_4^{2-}	H_2O	1.88×10^4/ 4.1×10^3/ 3.9×10^3	-	*S2*
Tb-TCPP	Fe^{3+}/Al^{3+}/ Cr^{3+}	DMF	-	16.4 nM/7.79 nM/ 9.94 nM	*S3*
$[Eu(Hpzbc)_2(NO_3)]\cdot H_2O$	Fe^{3+}/ $Cr_2O_7^{2-}$	EtOH	-	2.6×10^{-5} M/ 2.2×10^{-5} M	*S4*
$[Tb_4(\mu_6\text{-}L)_2(\mu\text{-}HCOO)(\mu_3\text{-}OH)_3(\mu_3\text{-}O)(DMF)_2(H_2O)_4]_n\cdot (H_2O)_{4n}$	Fe^{3+}/Ce^{3+}/ acetone	DMF	16590/279.4/-	10^{-6} M/-/-	*S5*
$[Eu(L)(HCOO)(H_2O)]_n$	$Cr_2O_7^{2-}$/CrO_4^{2-}	H_2O	2762.6/1537.4	1.0 μM /1.2 μM	*S6*
$[Tb(TBOT)(H_2O)](H_2O)_4(DMF)(NMP)_{0.5}$	Fe^{3+}/ $Cr_2O_7^{2-}$/ MnO_4^-/ 4-NT	H_2O	5.51×10^3/ 1.37×10^4/ 6.63×10^4/ 7.90×10^4	0.13 mM/ 0.14 mM/ 0.34 mM 0.32 mM	*S7*
$[Tb(ppda)(bdc)_{0.5}(C_2H_5OH)(H_2O)]_n$	Fe^{3+}/ $Cr_2O_7^{2-}$/ TNP	DMF	2.10×10^4/ 4.03×10^3/ 1.55×10^5	1.0×10^{-5} M/ 5.0×10^{-5} M/ 3.0×10^{-8} M	*S8*
$[Eu_2(2,3'\text{-}oba)_3(phen)_2]_n$	Fe^{3+}/ $Cr_2O_7^{2-}$/ CrO_4^{2-}/ MDZ	H_2O	1.37×10^4/ 2.17×10^4/ 1.59×10^4/ 2.39×10^4	7.93 uM/ 3.79 uM/ 2.4 uM/ 2.75 uM	*S9*
$\{[Eu_4(INO)_5(\mu_3\text{-}OH)_2Cl_4(H_2O)]\cdot(NO_3)\cdot(H_2O)_5\}_n$	$Cr_2O_7^{2-}$/ TNP/ NB/ PNT/ PNP	H_2O	-/ 0.92×10^3/ 0.30×10^3/ 3.54×10^3/ 9.34×10^4	-/ 0.03 mM/ 0.04 mM/ 0.09 mM/ 0.08 mM	*S10*
$[Eu_2(ppda)_2(npdc)(H_2O)]\cdot H_2O$	Fe^{3+}/ Cr^{3+}/ Al^{3+}/ PO_4^{3-}/ TNP	H_2O	1.64×10^5/ 1.98×10^6/ 8.68×10^5/ 1.8×10^5/ 3.44×10^5	1.66×10^{-5} M/ 6.17×10^{-5} M/ 1.09×10^{-4} M/ 1.42×10^{-5} M/ 2.97×10^{-6} M	*S11*
$[Zr_6(\mu_3\text{-}O)_4(\mu_3\text{-}OH)_4(OH)_4(H_2O)_4(L)_2]\cdot 3H_2O\cdot 2DMF$	Fe^{3+}/ $Cr_2O_7^{2-}$/ PA	H_2O/ H_2O/ DMSO	6.51×10^6/ 1.02×10^6/ 4.56×10^5	3.75 ppb/ 8.58 ppb/ 13.08 ppb	*S12*
$[Tb(Hpta)(C_2O_4)]\cdot 3H_2O(3)$	Fe^{3+}/ $Cr_2O_7^{2-}$/ NIF	H_2O/ H_2O/ DMF	1.22×10^4/ 1.02×10^4/ 1.1×10^4	2.6×10^{-5} M/ 3.8×10^{-5} M/ 8.1×10^{-5} M	*S13*
$\{[Eu_2L_{1.5}(H_2O)_2EtOH]\cdot DMF\}_n$	Fe^{3+}/ $Cr_2O_7^{2-}$/PA	DMF	2942/1526/ 2001	1×10^{-5} M/ 1×10^{-5} M/ 1×10^{-5} M	*S14*
$\{[Eu(dpc)(2H_2O)]\cdot (Hbibp)_{0.5}\}_n$	Fe^{3+}/ $Cr_2O_7^{2-}$/ Cu^{2+}/ NB	DMF	4.84×10^3/ 3.97×10^3/ 4.62×10^3/ 3.34×10^3	1.32×10^{-5} M/ 1.01×10^{-5} M/ 2.53×10^{-5} M/ 2.89×10^{-5} M	*S15*
$[Ln(L^{2-})(HL^-)(H_2O)_2]_n$	Fe^{3+}/ 2,4-DNP	H_2O/ EtOH	6.16×10^3/ 1.28×10^4	0.17 uM/ 16.4 uM	*S16*
Eu(O-cpia)(phen)	Fe^{3+}/ PO_4^{3-}/ F^-	H_2O	-	300 ppm/ 100 ppm/ 100 ppm	*S17*

Table S2 Selected bond lengths (Å) and angles (°) for **DPQ-Eu**.

DPQ-Eu					
Bond Lengths (Å)					
Eu1-O1[1]	2.456(2)	Eu1-O2	2.290(2)	Eu1-O3	2.376(3)
Eu1-O3[2]	2.532(2)	Eu1-O4[2]	2.583(4)	Eu1-O5	2.479(3)
Eu1-O6[3]	2.381(3)	Eu1-O7[1]	2.552(3)	Eu1-O10	2.534(3)
Bond Angles (°)					
O1[1]-Eu1-O3[2]	107.17(7)	O1[1]-Eu1-O4[2]	76.18(9)	O1[1]-Eu1-O5	125.29(8)
O1[1]-Eu1-O7[1]	52.03(7)	O1[1]-Eu1-O10	143.98(8)	O2-Eu1-O1[1]	74.30(10)
O2-Eu1-O3	145.93(7)	O2-Eu1-O3[2]	128.56(8)	O2-Eu1-O4[2]	82.29(9)
O2-Eu1-O5	73.67(11)	O2-Eu1-O6[3]	105.90(9)	O2-Eu1-O7[1]	125.84(8)
O2-Eu1-O10	79.64(9)	O3-Eu1-O1[1]	136.87(8)	O3-Eu1-O3[2]	64.18(10)
O3[2]-Eu1-O4[2]	50.56(6)	O3-Eu1-O4[2]	114.20(10)	O3-Eu1-O5	75.19(10)
O3-Eu1-O6[3]	76.65(10)	O3-Eu1-O7[1]	87.59(7)	O3[2]-Eu1-O7[1]	70.04(6)
O3-Eu1-O10	76.25(7)	O3[2]-Eu1-O10	70.91(7)	O5-Eu1-O3[2]	127.49(6)
O5-Eu1-O4[2]	139.62(9)	O5-Eu1-O7[1]	141.50(8)	O5-Eu1-O10	68.15(9)
O6[3]-Eu1-O1[1]	76.06(12)	O6[3]-Eu1-O3[2]	124.71(7)	O6[3]-Eu1-O4[2]	147.53(8)
O6[3]-Eu1-O5	71.70(12)	O6[3]-Eu1-O7[1]	70.91(10)	O6[3]-Eu1-O10	135.92(9)
O7[1]-Eu1-O4[2]	78.83(8)	O10-Eu1-O4[2]	76.05(8)	O10-Eu1-O7[1]	140.95(8)

symmetry code: [1]1-X, +Y, 3/2-Z; [2]1-X, -Y, 1-Z; [3]1-X, 1-Y, 1-Z

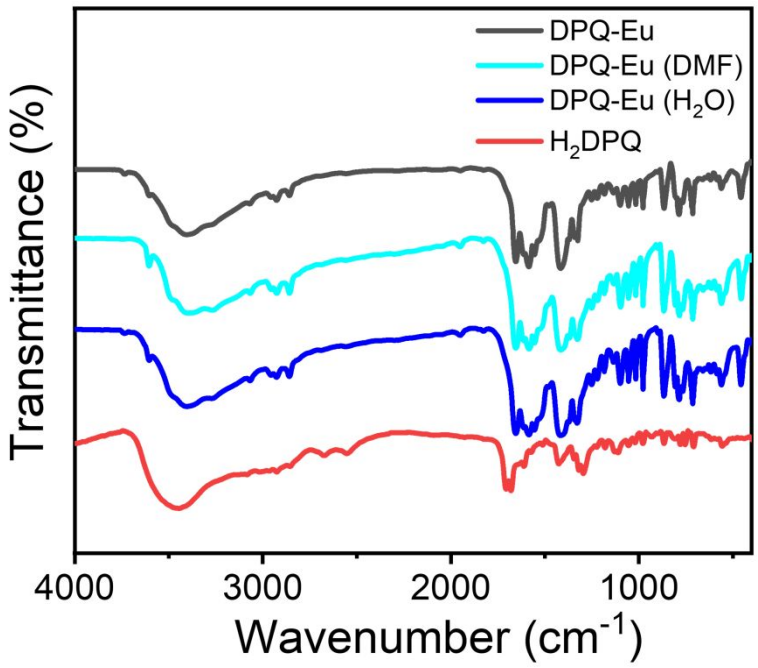

Figure S1 IR spectra of **H_2DPQ**, **DPQ-Eu**, and **DPQ-Eu** immersed in H_2O and DMF for 24 h. (IR (KBr, cm^{-1}): **H_2DPQ**: 3450 (m), 2671 (w), 2549 (w), 1706 (s), 1679 (s), 1606 (w), 1422 (w), 1350 (w), 1313 (w), 1291 (w), 1182 (w), 1128 (w), 1056 (w), 1020 (w), 966 (w), 870 (w), 780 (w), 752 (w), 704 (w); **DPQ-Eu**: 3452 (m), 2929 (w), 1656 (m), 1581 (m), 1417 (s), 1332 (w), 1087 (w), 977 (w), 863 (w), 788 (w), 717 (w).)

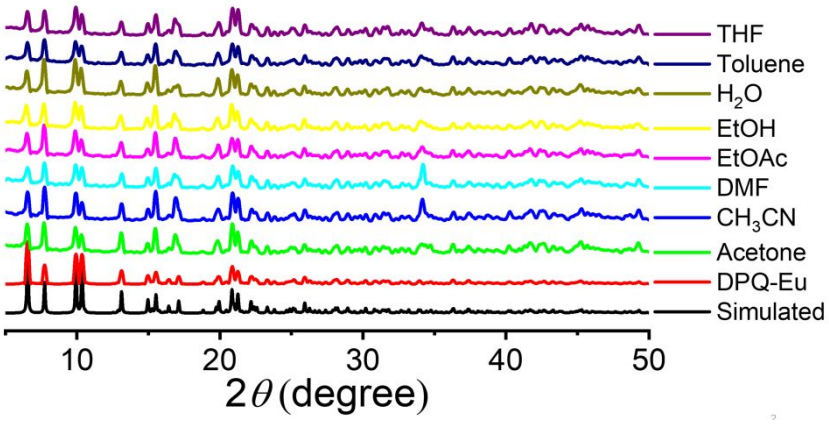

Figure S2 PXRD patterns for **DPQ-Eu** immersed in commonly used solvents for 24 h.

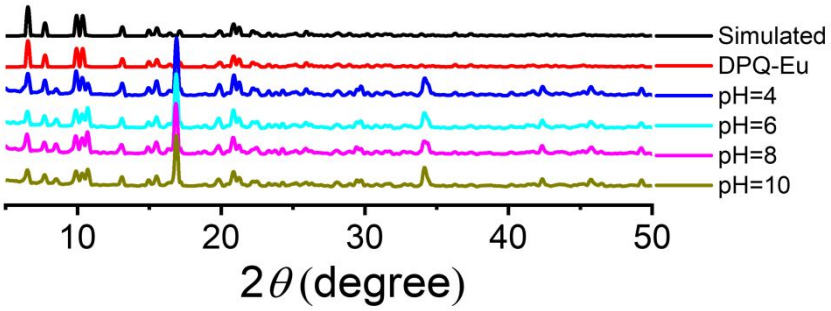

Figure S3 PXRD patterns for **DPQ-Eu** immersed in water with different pH values for 24 h.

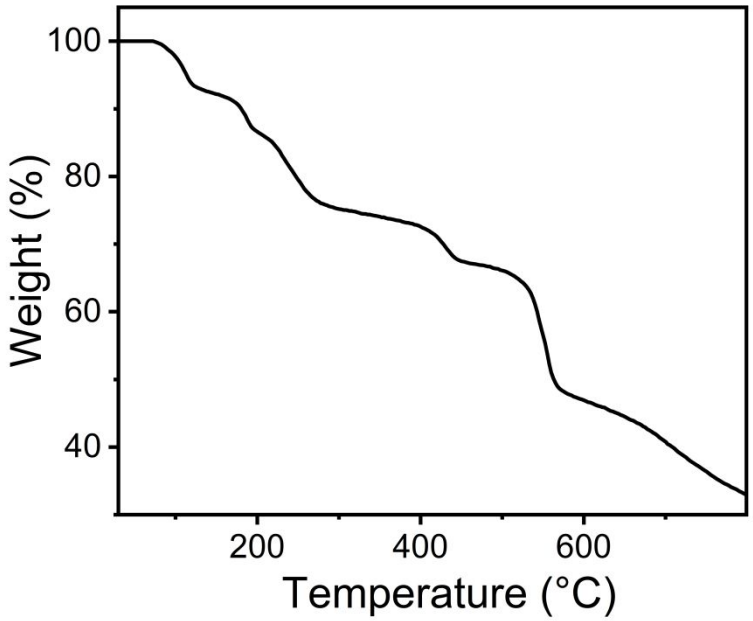

Figure S4 TG curve of **DPQ-Eu**.

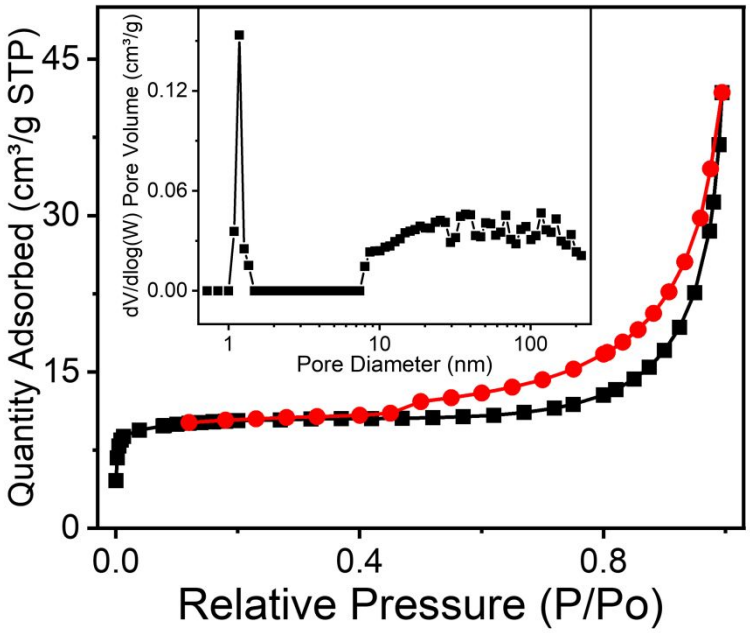

Figure S5 N_2 adsorption-desorption isotherms of **DPQ-Eu** at 77 K and pore size distribution.

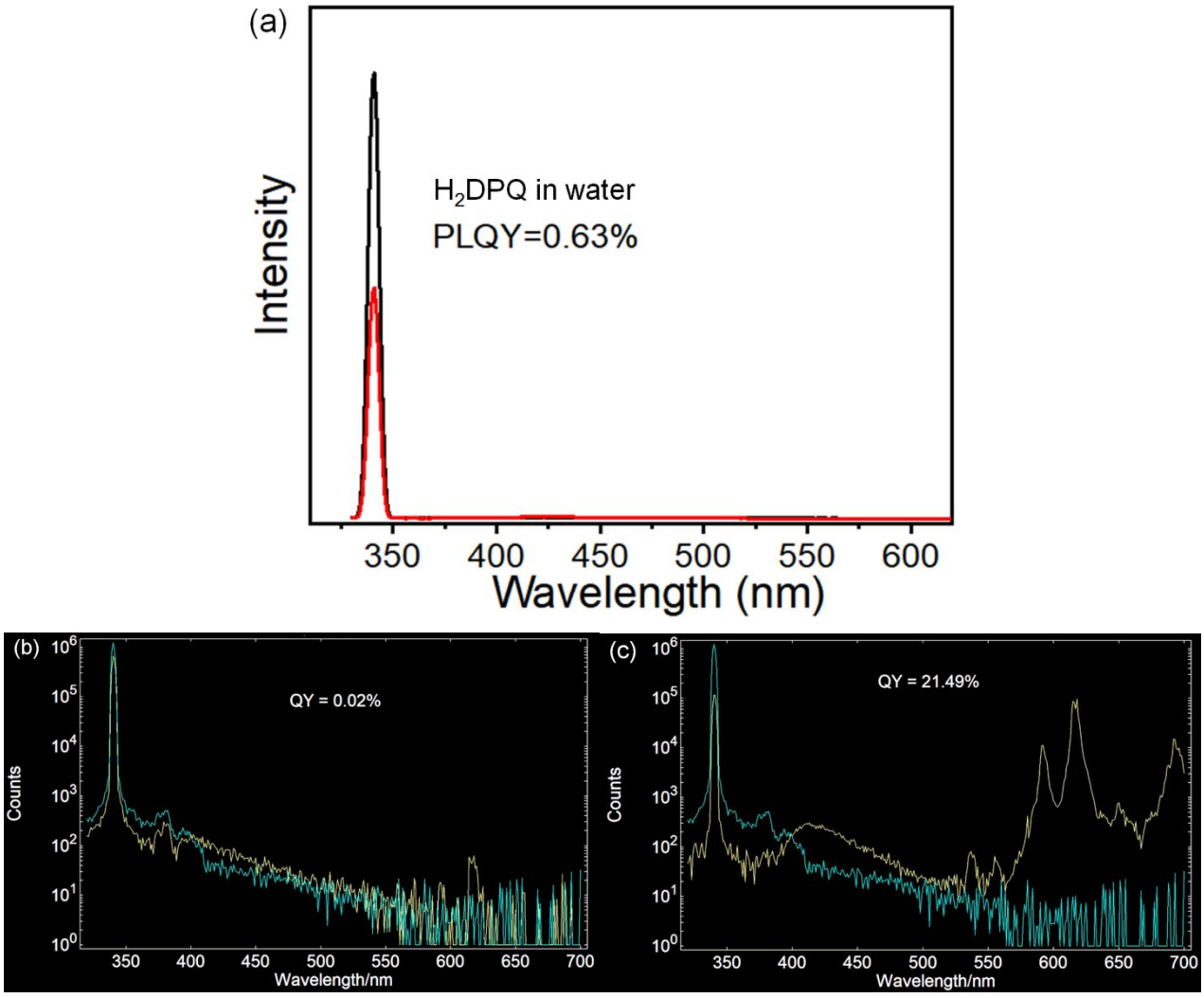

Figure S6 Absolute quantum efficiency of **H_2DPQ** in (a) water, (b) at solid state, and (c) solid **DPQ-Eu**.

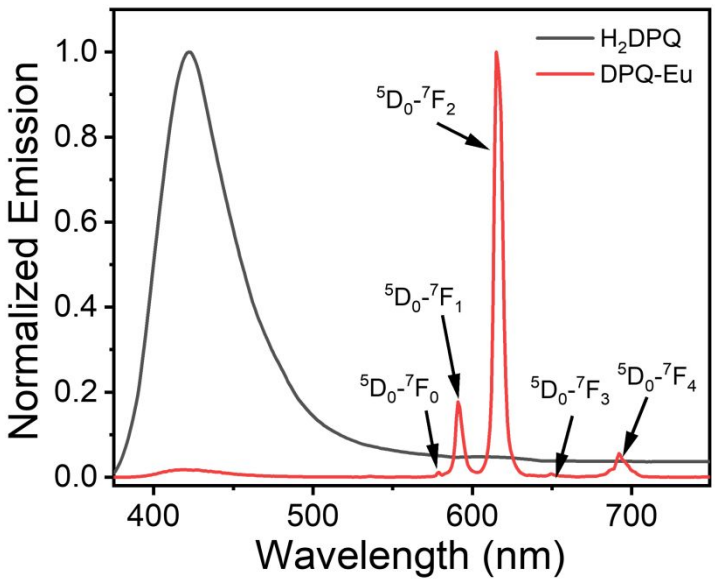

Figure S7 Emission spectra of **H_2DPQ** and **DPQ-Eu**.

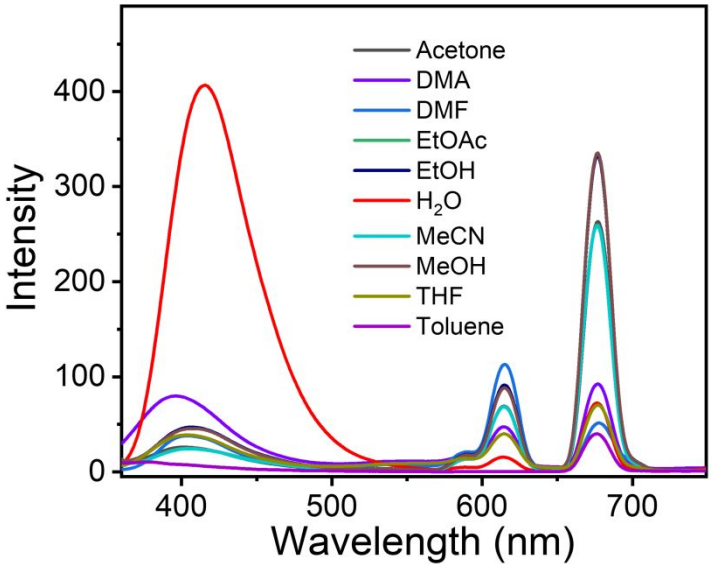

Figure S8 Emission spectra of **DPQ-Eu** (0.1 mg/3 mL) in different solvents.

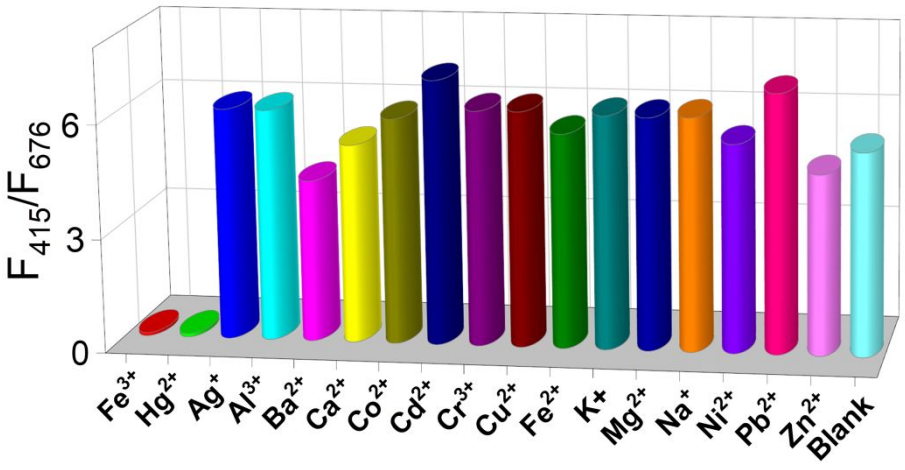

Figure S9 Fluorescent selectivity to various metal ions (185 μM).

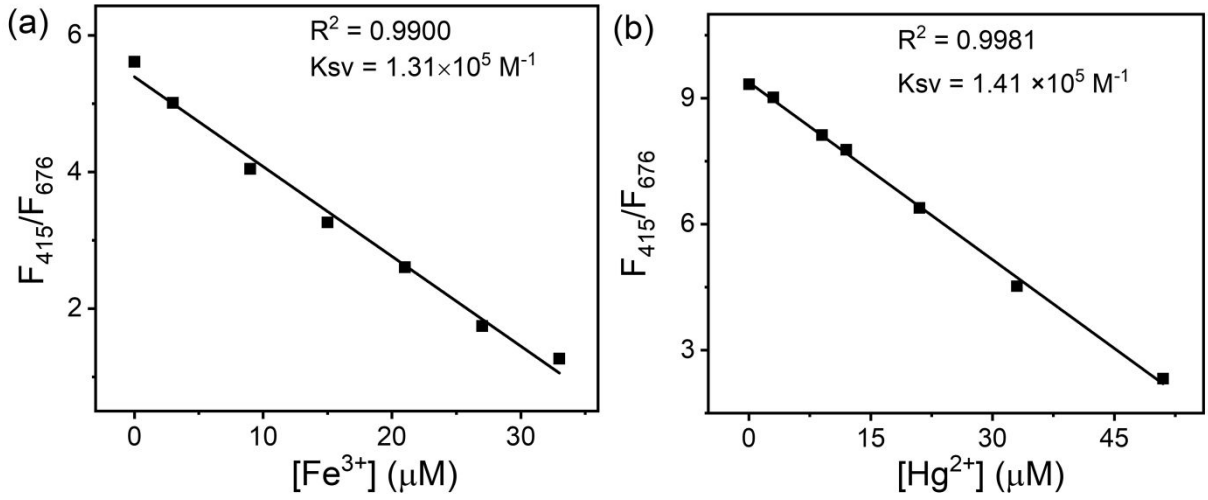

Figure S10 Stern-Volmer curves of **DPQ-Eu** towards (a) Fe^{3+} and (b) Hg^{2+}.

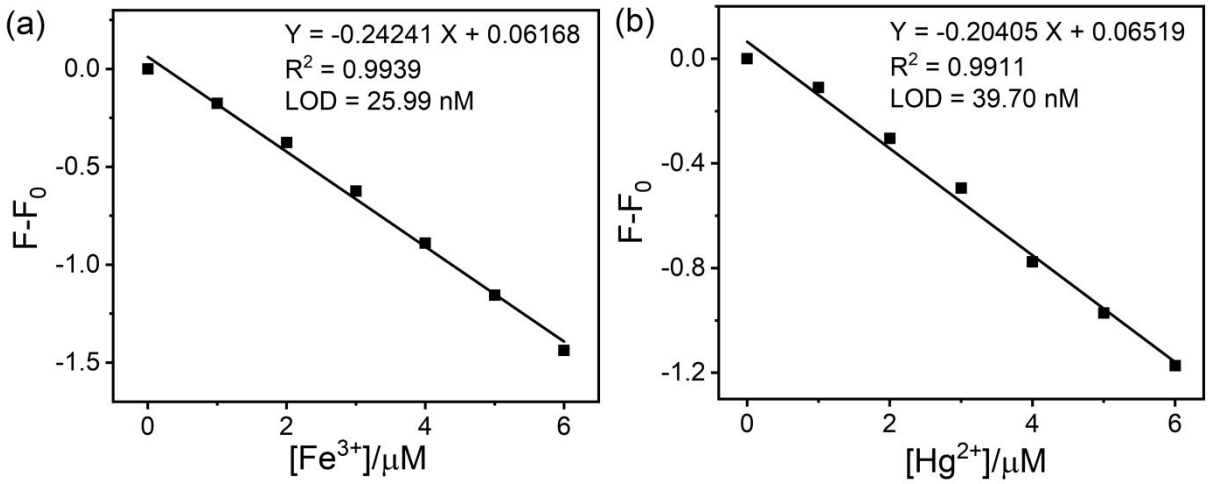

Figure S11 The detection limits of **DPQ-Eu** towards (a) Fe^{3+} (n = 10, σ = 0.0021) and (b) Hg^{2+} (n = 10, σ = 0.0027) by 3σ/k in water, where σ is the standard deviation of blank measurement, k is the slope, λ_{ex}: 340 nm.

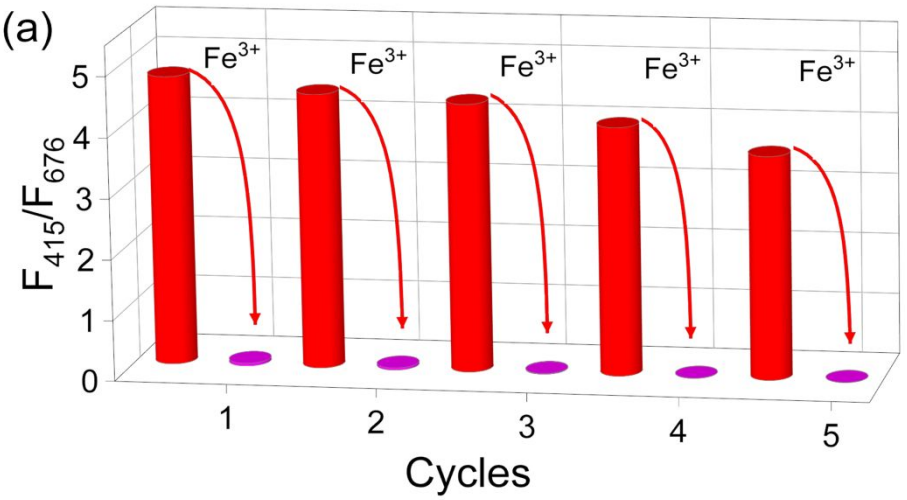

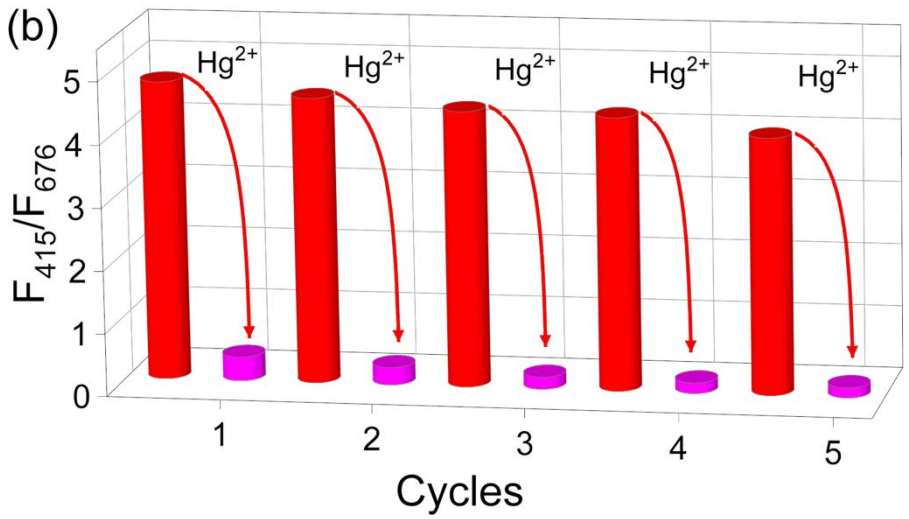

Figure S12 Recyclable experiments of **DPQ-Eu** for sensing of (a) Fe^{3+} (157 μM) and (b) Hg^{2+} (185 μM).

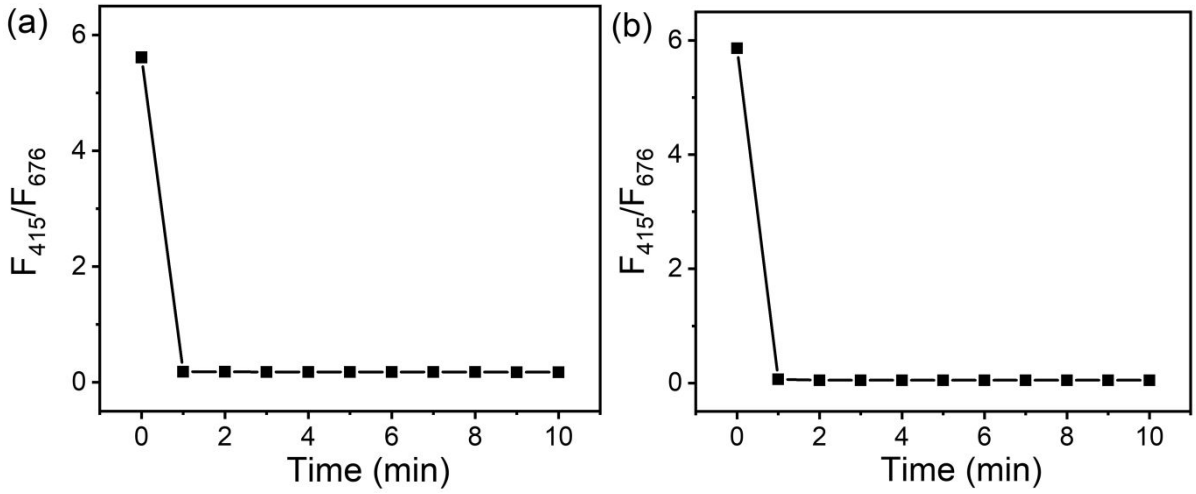

Figure S13 Emission ratios intensity of **DPQ-Eu** treated by (a) Fe^{3+} (157 μM) and (b) Hg^{2+} (185 μM) as a function of time, λ_{ex}: 340 nm.

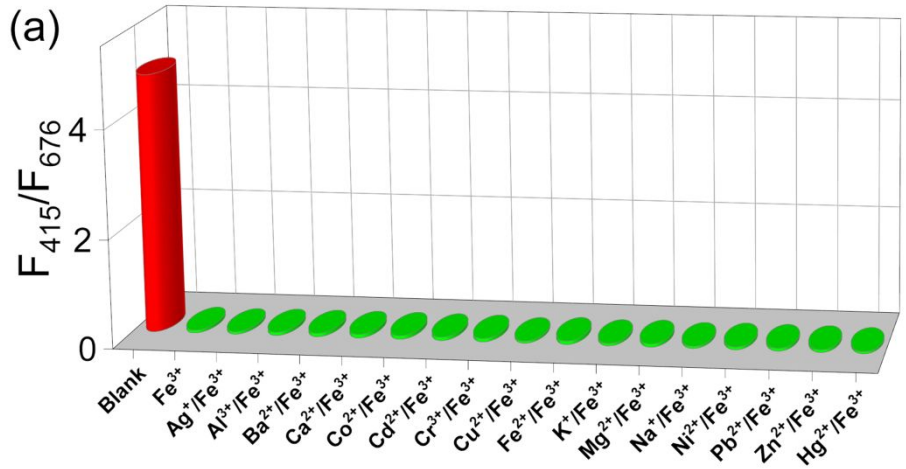

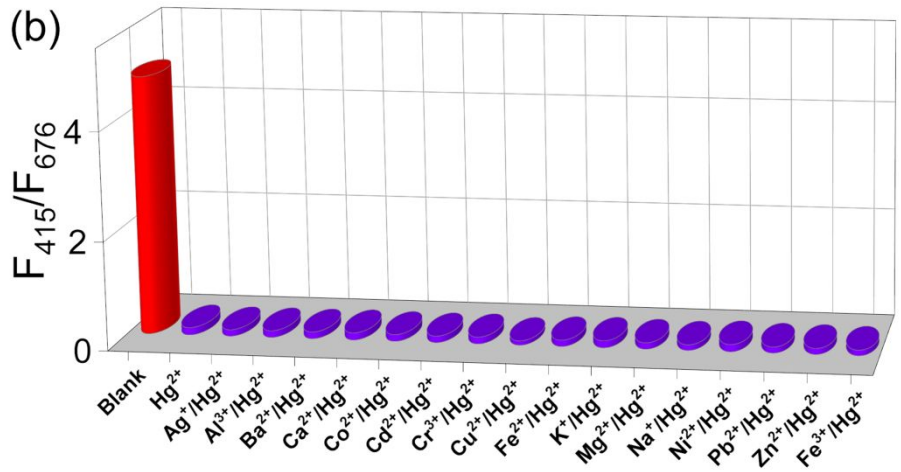

Figure S14 Emission ratios intensity of the **DPQ-Eu** dispersed in the mixture of other metal ions and (a) Fe^{3+} (157 μM) / (b) Hg^{2+} (185 μM), λ_{ex}: 340 nm.

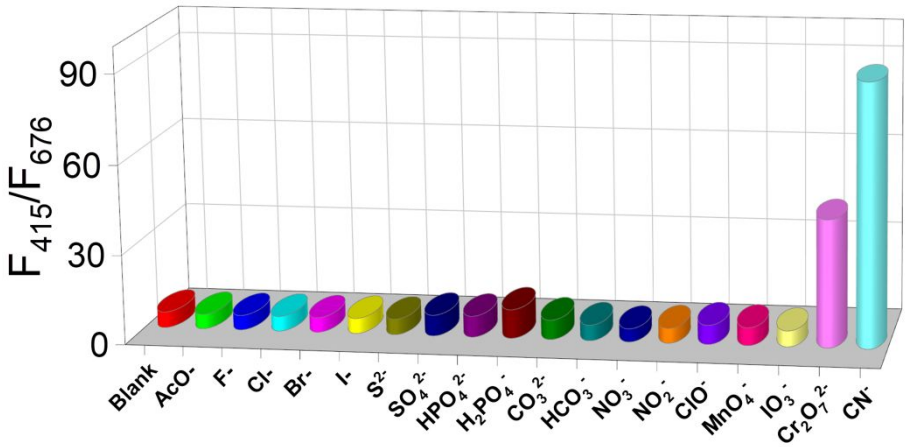

Figure S15 Selectivity experiment to various anions (190 μM).

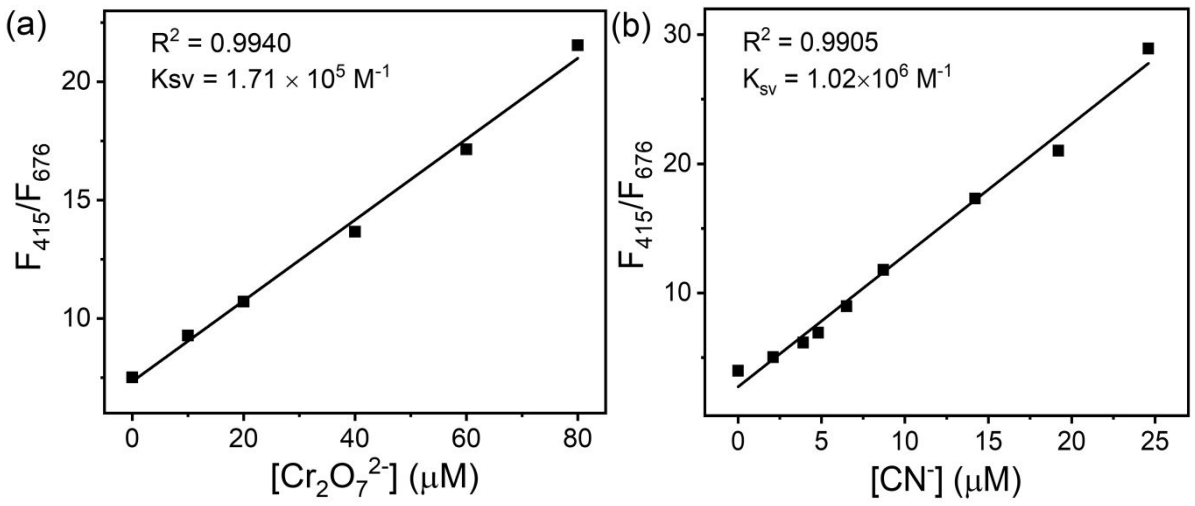

Figure S16 SV curves of **DPQ-Eu** towards (a) $Cr_2O_7^{2-}$ and (b) CN^- anions, λ_{ex}: 340 nm.

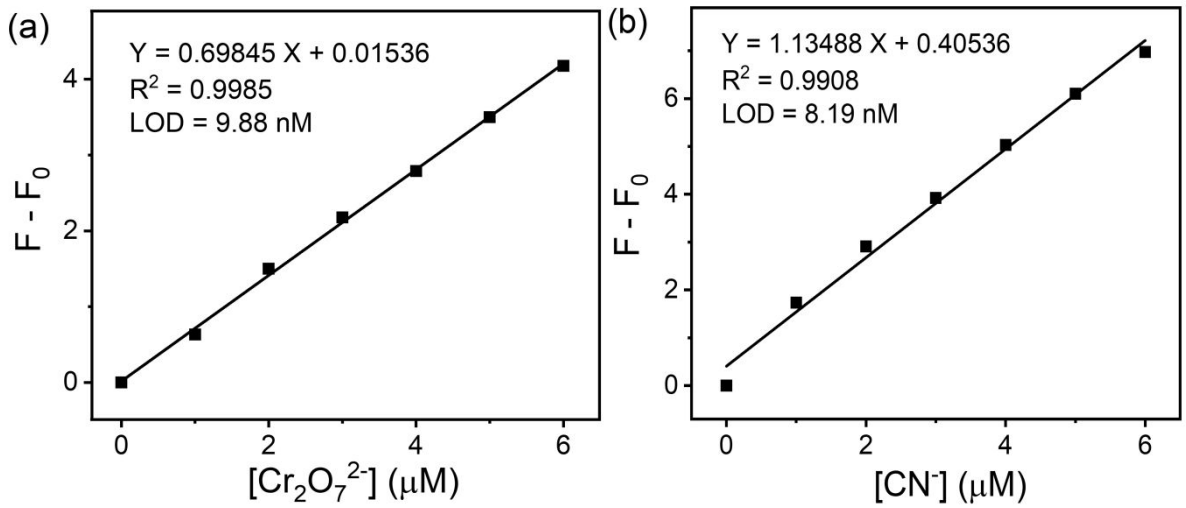

Figure S17 The detection limits of **DPQ-Eu** towards (a) $Cr_2O_7^{2-}$ (n = 10, σ = 0.0023) and (b) CN^- (n = 10, σ = 0.0031) by 3σ/k in water, where σ is the standard deviation of blank measurement, k is the slope, λ_{ex}: 340 nm.

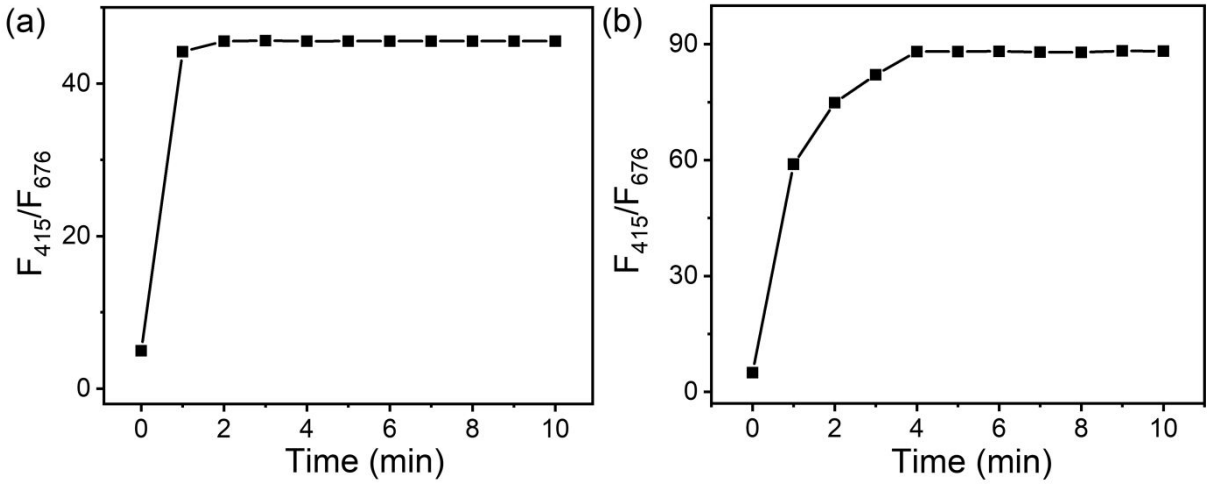

Figure S18 Emission ratios intensity of **DPQ-Eu** treated by (a) $Cr_2O_7^{2-}$ (190 μM) and (b) CN^- (53.3 μM) as a function of time, λ_{ex}: 340 nm.

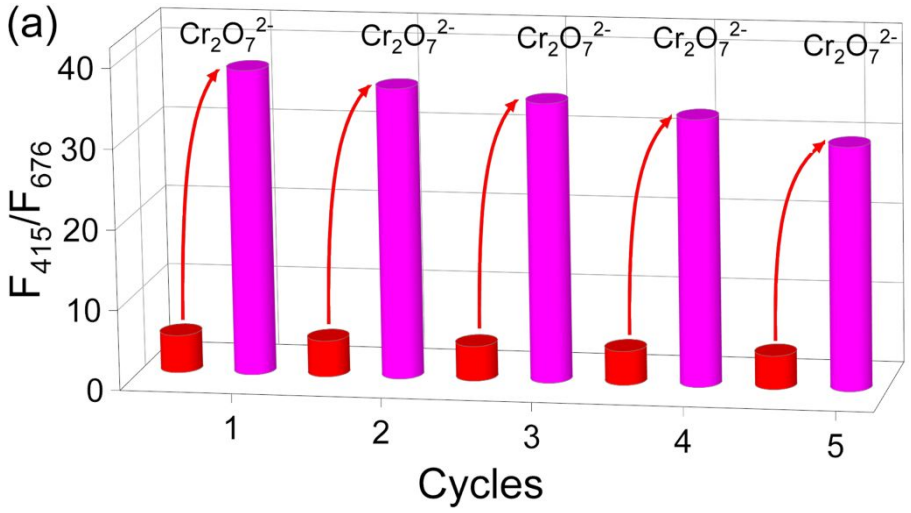

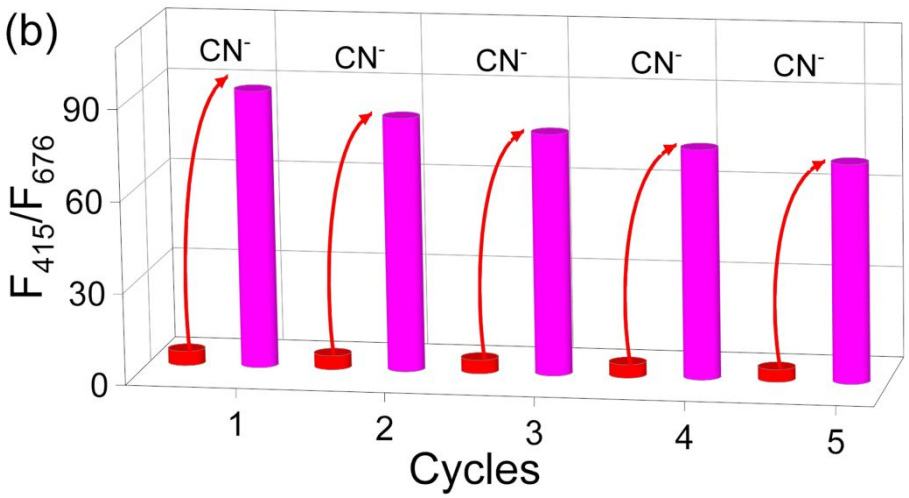

Figure S19 Recyclable experiments of **DPQ-Eu** for sensing of (a) $Cr_2O_7^{2-}$ (190 μM) and (b) CN^- (53.3 μM).

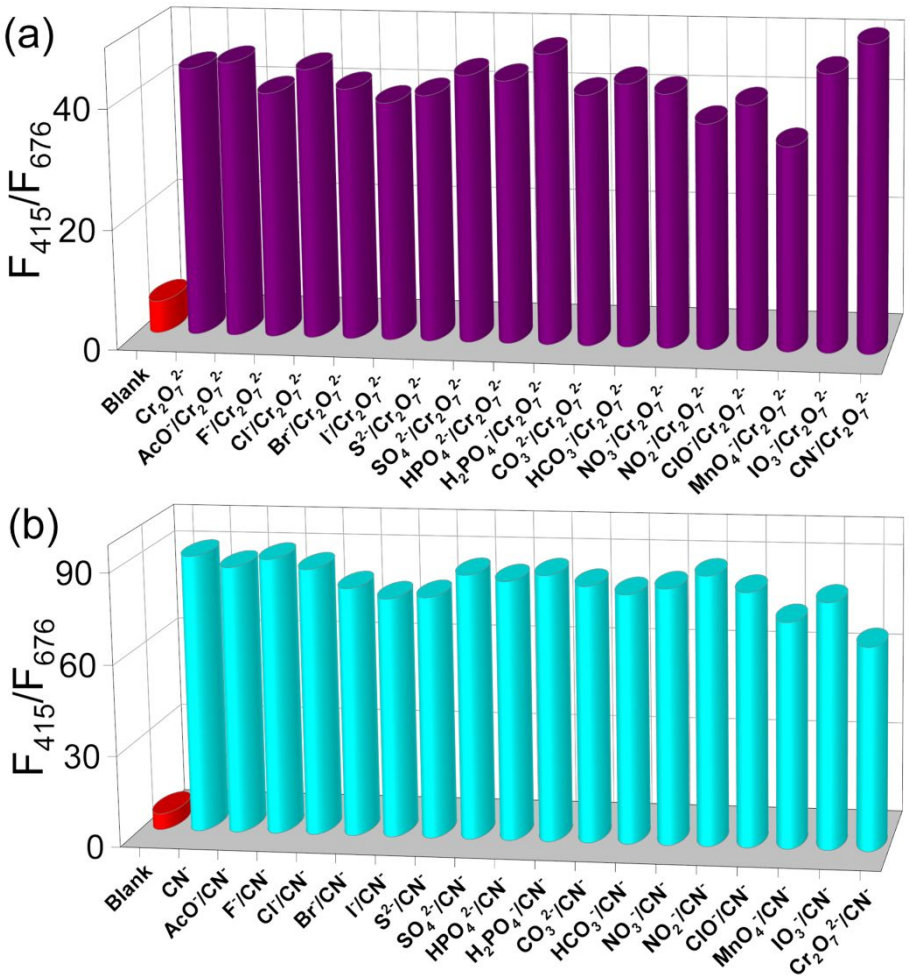

Figure S20 Emission ratios intensity of the **DPQ-Eu** dispersed in the mixture of other anions and (a) $Cr_2O_7^{2-}$ (190 μM) / (b) CN^- (53.3 μM), λ_{ex}: 340 nm.

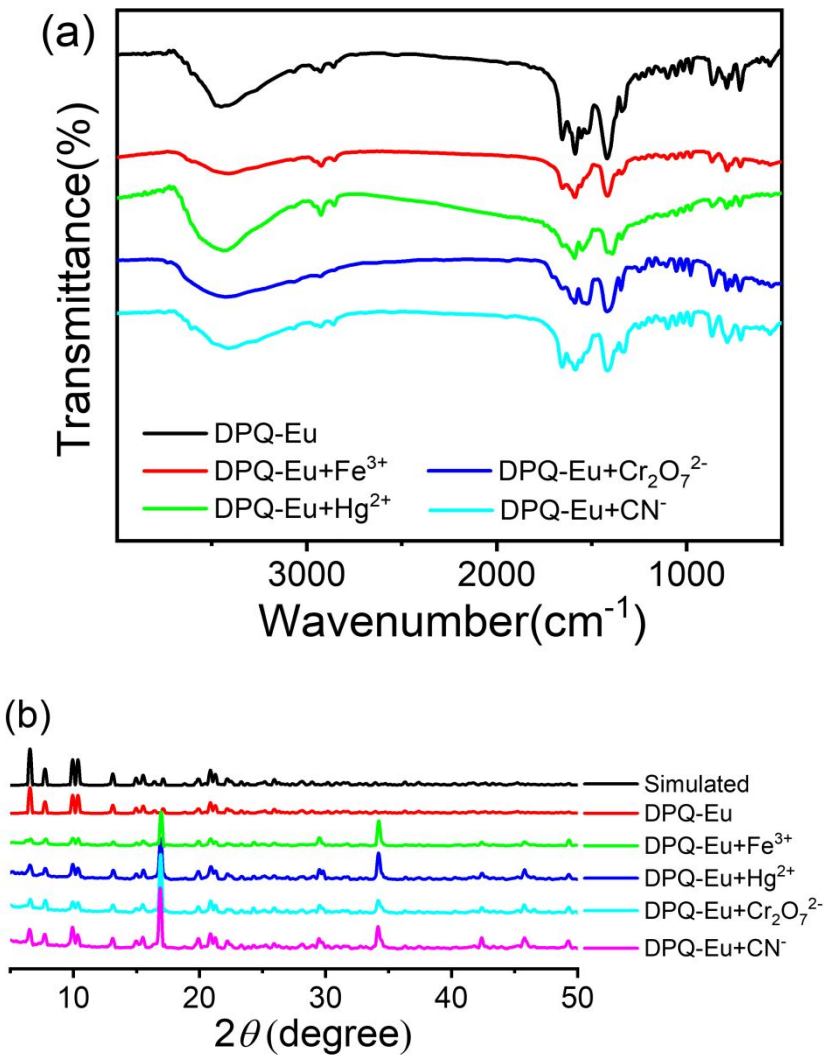

Figure S21 (a) IR spectra and (b) PXRD patterns of **DPQ-Eu** immersed in Fe^{3+}, Hg^{2+}, $Cr_2O_7^{2-}$ and CN^- for 24 h. (IR (KBr, cm^{-1}): **DPQ-Eu**: 3452 (m), 2929 (w), 1656 (m), 1581 (m), 1417 (s), 1332 (w), 1087 (w), 977 (w), 863 (w), 788 (w), 717 (w); **DPQ-Eu+Fe^{3+}**: 3412 (m), 2916 (w), 2854 (w), 1654 (m), 1582 (m), 1416 (m), 1334 (w), 109**6** (w), 972 (w), 868 (w), 786 (w), 713 (w); **DPQ-Eu+Hg^{2+}**: 3412 (m), 2926 (w), 2854 (w), 1660 (m), 1587 (m), 1556 (w), 1422 (m), 1329 (w), 1050 (w), 977 (w), 863 (w), 791 (w), 719 (w); **DPQ-Eu+$Cr_2O_7^{2-}$**: 3442 (m), 2925 (w), 2853 (w), 1653 (w), 1591 (m), 1550 (w), 1416 (m), 1343 (w), 1054 (w), 981 (w), 867 (w), 785 (w), 723 (w); **DPQ-Eu+CN^-**: 3402 (m), 3061 (w), 2926 (w), 1706 (m), 1665 (w), 1592 (m), 1530 (m), 1416 (m), 1344 (w), 1054 (w), 982 (w), 858 (w), 786 (w), 713 (w).)

Table S3 The ICP-MS analysis of **DPQ-Eu** and ICP-MS analysis of **DPQ-Eu** immersed in Fe^{3+} (157 μM) / Hg^{2+} (185 μM) for 24 h.

Samples	Eu^{3+} (mol/L)	Fe^{3+} (mol/L)-	Hg^{2+} (mol/L)
DPQ-Eu	21.89% (wt%)	-	
Filtrate of DPQ-Eu treated by Fe^{3+}	undetectable	5.4464×10^{-8}	-
Filtrate of DPQ-Eu treated by Hg^{2+}	undetectable	-	1.3184×10^{-8}

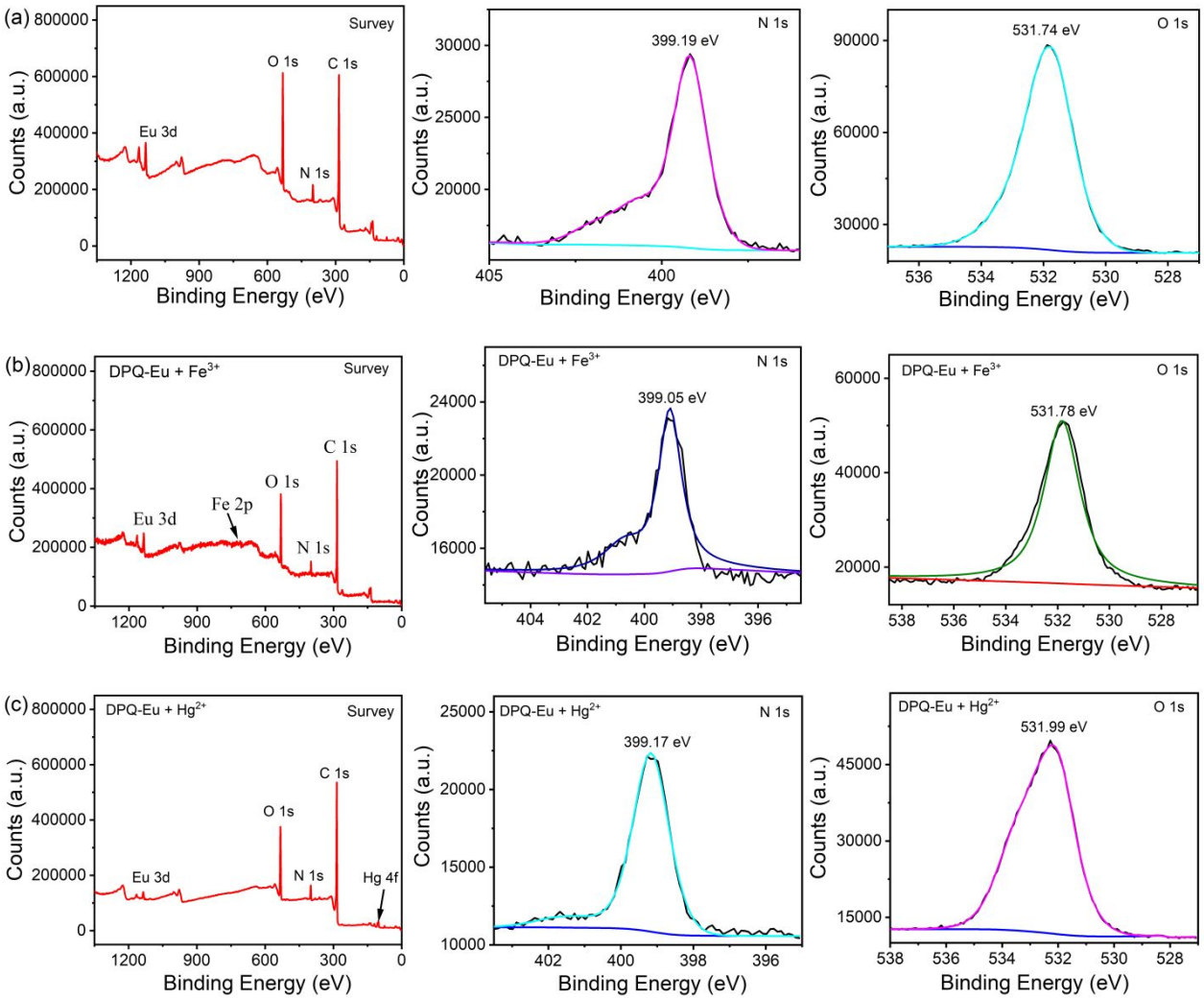

Figure S22 (a) XPS spectra of **DPQ-Eu**, (b) **DPQ-Eu** treated with Fe^{3+}, and (c) **DPQ-Eu** treated with Hg^{2+}. Overall spectra (left), N 1s (center), O1s (right).

Table S4 Binding energy of **DPQ-Eu** before and after treatment by Fe^{3+}/Hg^{2+}.

Survey	**DPQ-Eu**	**DPQ-Eu+Fe^{3+}**	**△BE (eV)**
N 1s	399.19	399.05	-0.14
O 1s	531.74	531.78	+0.04
Survey	**DPQ-Eu**	**DPQ-Eu+Hg^{2+}**	**△BE (eV)**
N 1s	399.19	399.17	-0.02
O 1s	531.74	531.99	+0.25

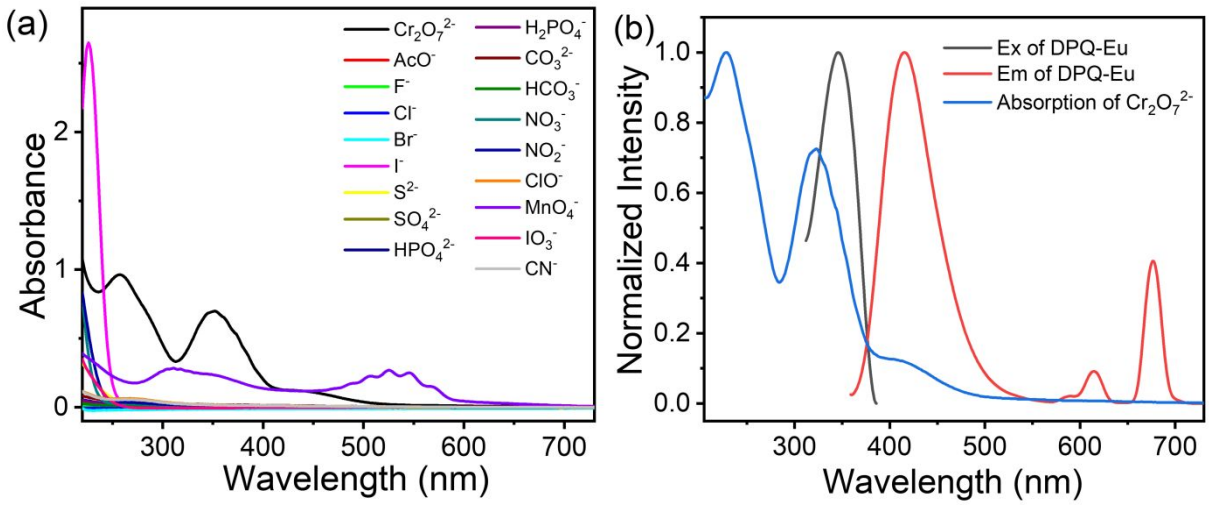

Figure S23 (a) Absorption spectra of various anions and (b) excitation and emission spectra of **DPQ-Eu** with the absorption of $Cr_2O_7^{2-}$.

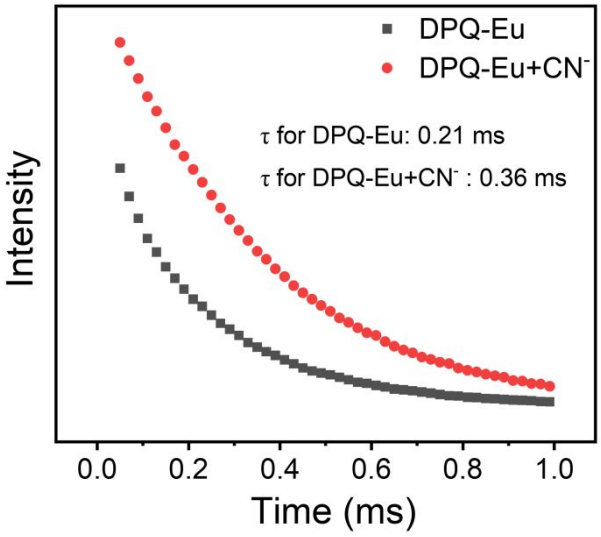

Figure S24 Fluorescence lifetime.

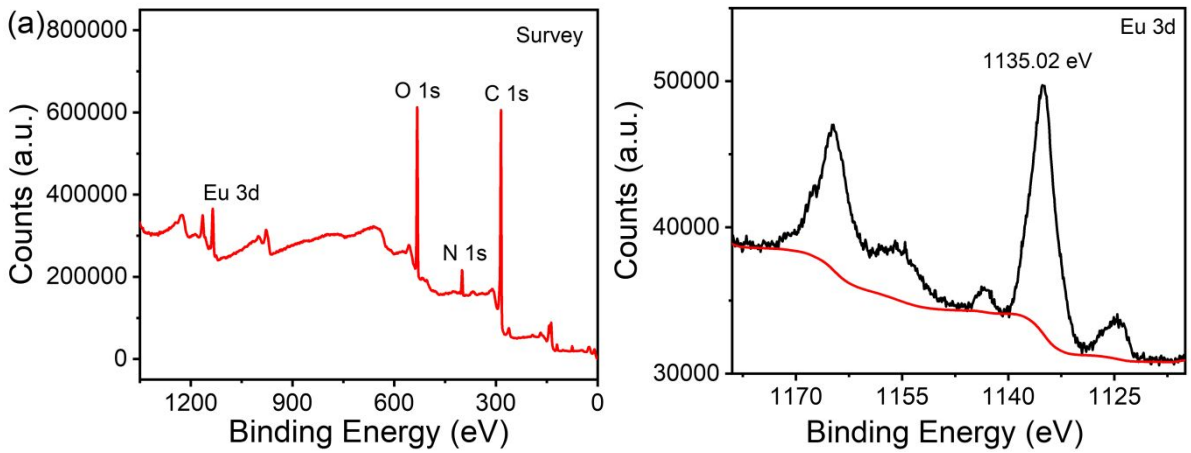

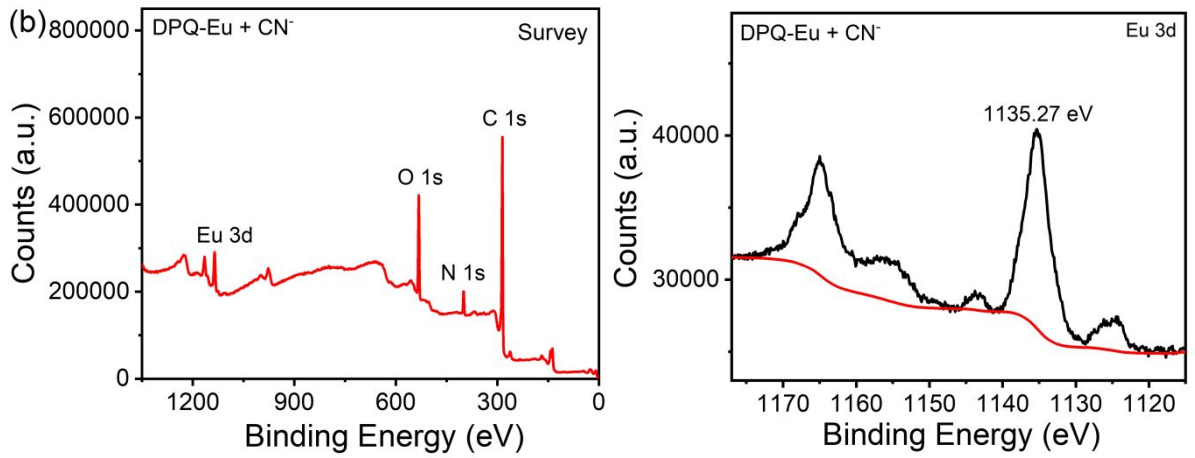

Figure S25 (a) XPS spectra of **DPQ-Eu**, (b) **DPQ-Eu** treated with CN^-. Overall spectra (left), Eu 3d (right).

Table S5 Binding energy of **DPQ-Eu** before and after treatment by CN^-.

Survey	DPQ-Eu	DPQ-Eu+CN^-	△BE (eV)
Eu 3d	1135.02	1135.27	+0.25

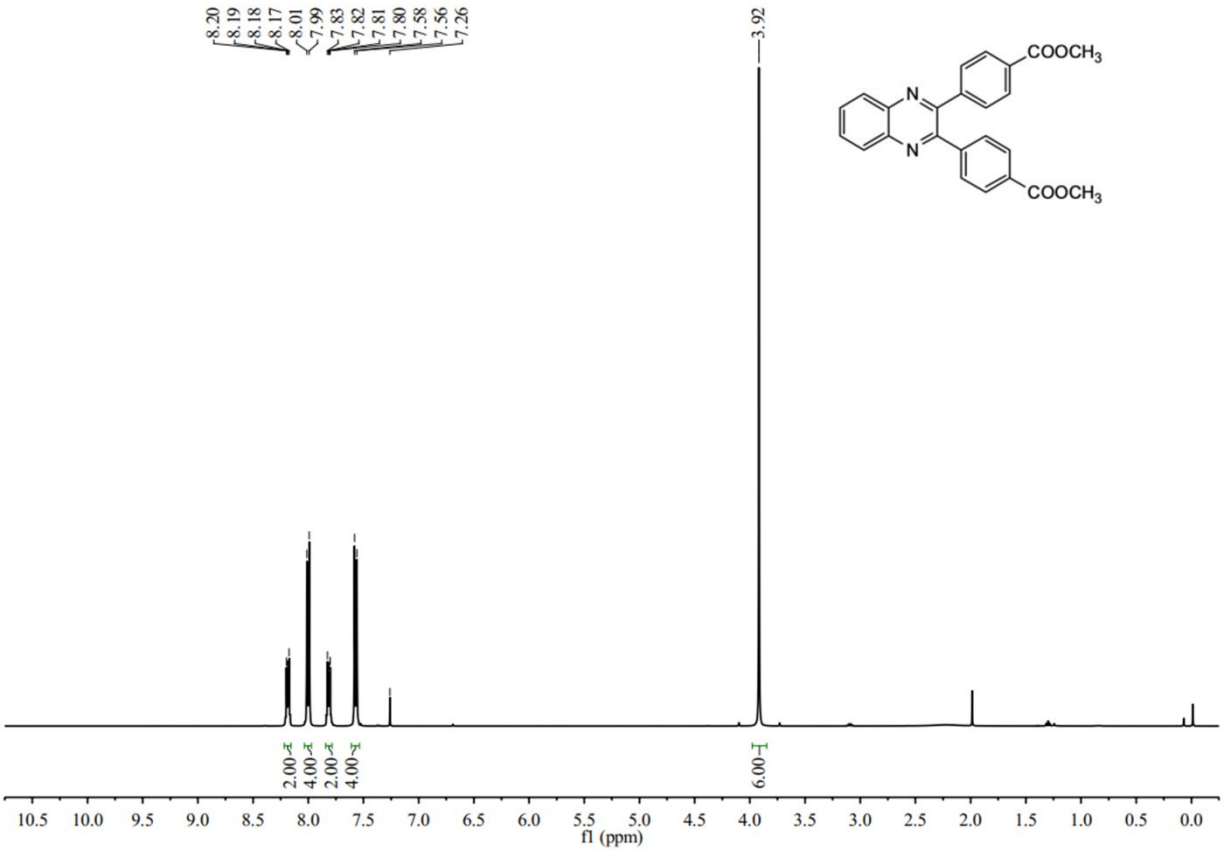

Figure S26 ^1H NMR (400 MHz) spectrum of **DPQMe** in $CDCl_3$.

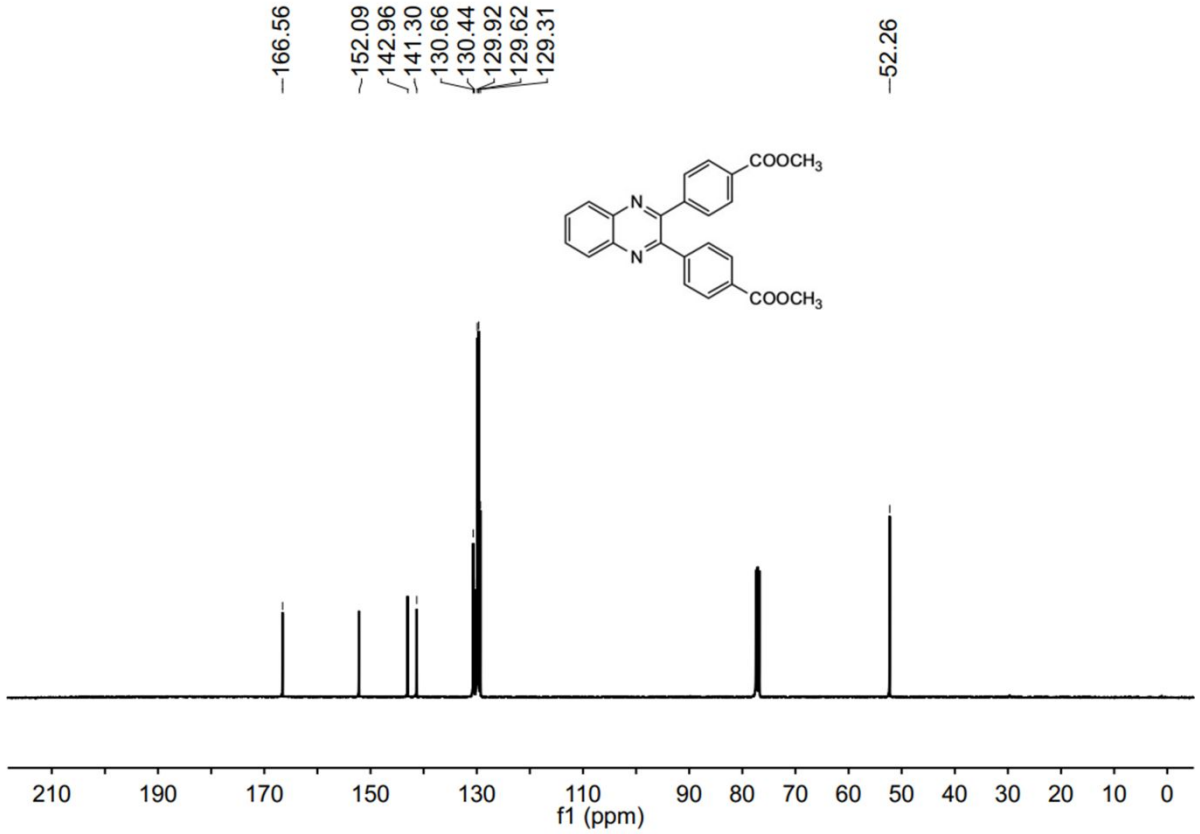

Figure S27 ^{13}C NMR (100 MHz) spectrum of **DPQMe** in $CDCl_3$.

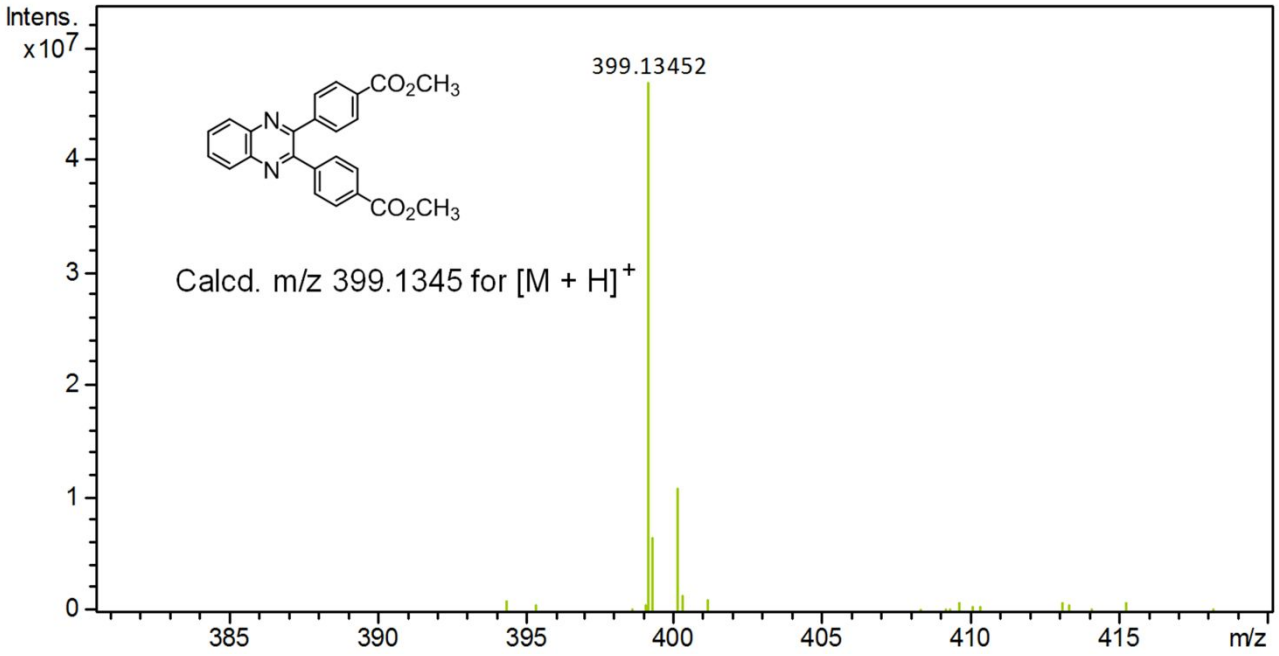

Figure S28 HRMS for **DPQMe**.

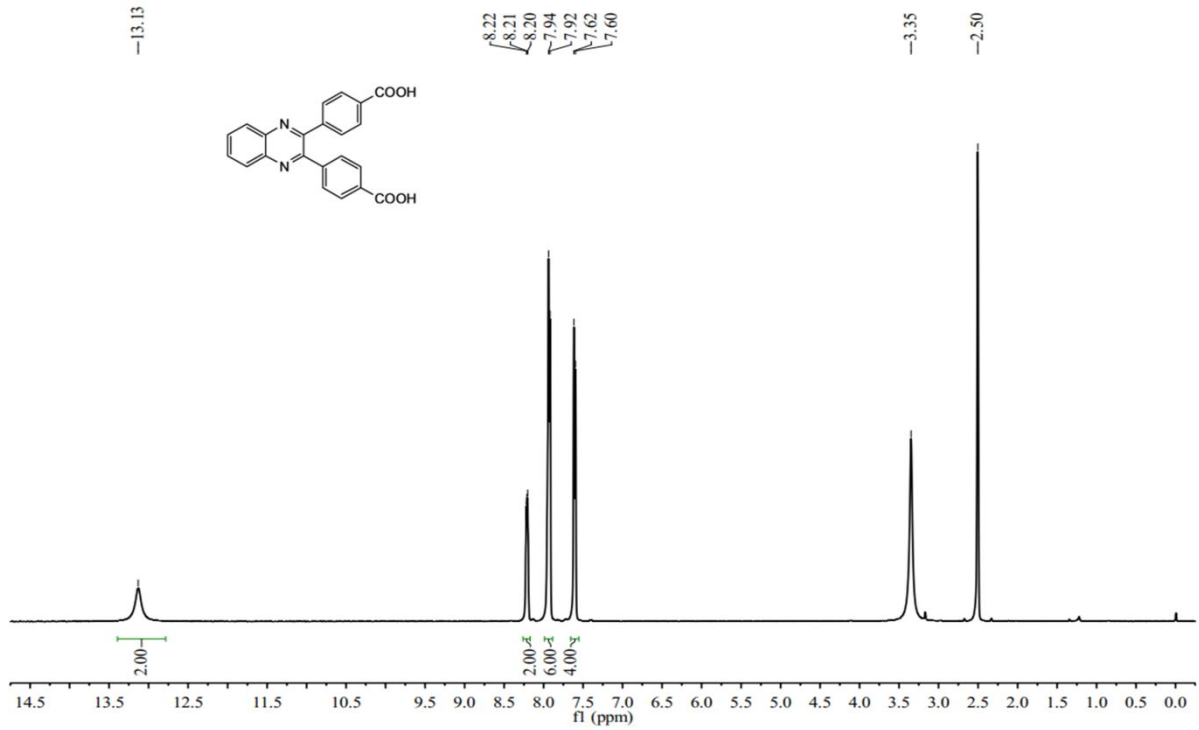

Figure S29 ^{1}H NMR (400 MHz) spectrum of **H_2DPQ** in DMSO-d_6.

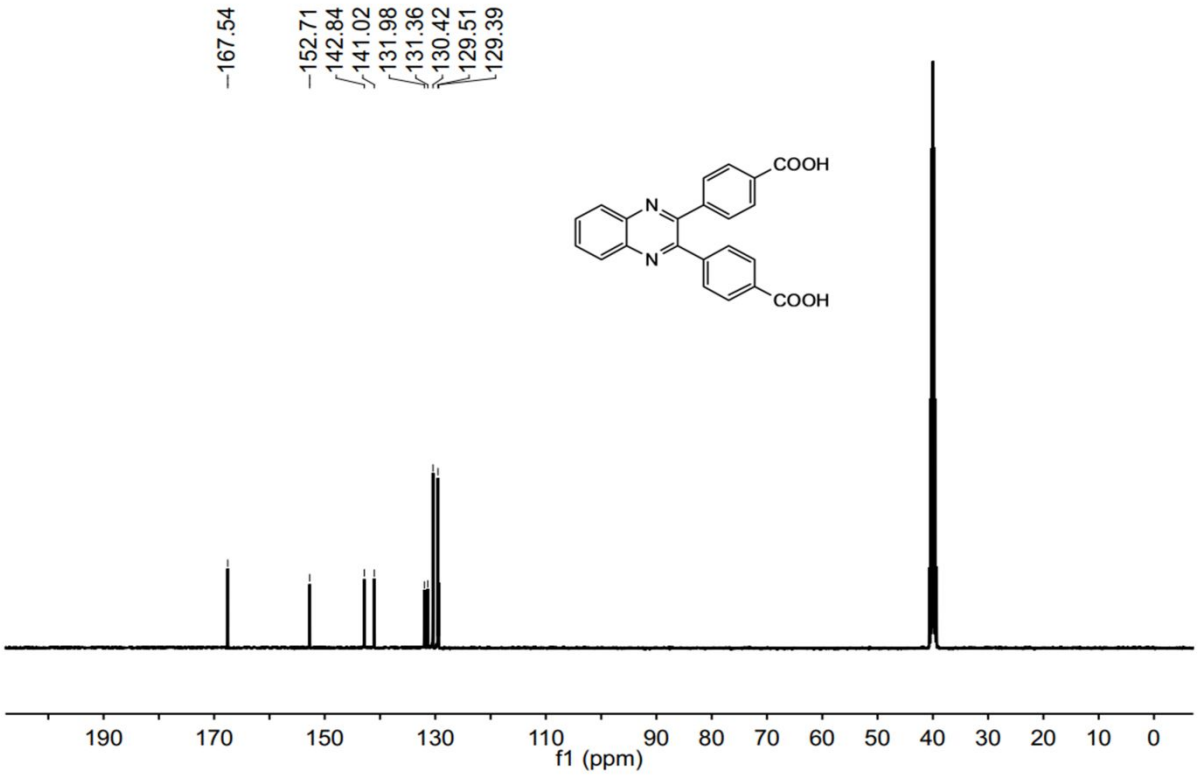

Figure S30 ^{13}C NMR (100 MHz) spectrum of **H_2DPQ** in DMSO-d_6.

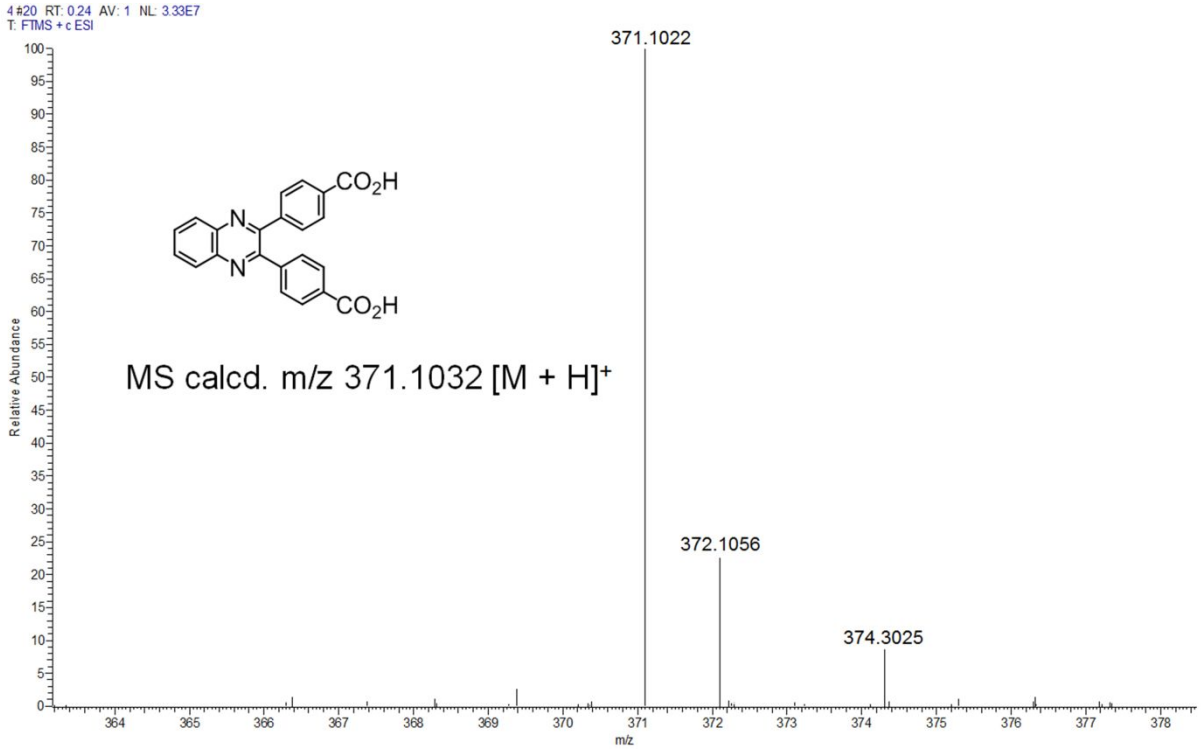

Figure S31 HRMS for **H_2DPQ**.

References

S1 Li, X.; Tang, J. X.; Liu, H.; Gao, K.; Meng, X. R.; Wu, J.; Hou, H. W. A highly sensitive and recyclable ln-mof luminescent sensor for the efficient detection of Fe^{3+} and Cr^{VI} anions. *Chem. - Asian. J.* **2019**, *14*, 3721.

S2. Wang, X. N.; Li, J. L.; Jiang, C. G.; Hu, P.; Li, B.; Zhang, T. L; Zhou, H. C. An efficient strategy for improving the luminescent sensing performance of a terbium (III) metal-organic framework towards multiple substances. *Chem. Commun.* **2018**, *54*, 13271-13274.

S3. Fu, C. C.; Sun, X. R.; Zhang, G. D.; Shi, P. H.; Cui, P. Porphyrin-based metal-organic framework probe: highly selective and sensitive fluorescent turn-on sensor for M^{3+} (Al^{3+}, Cr^{3+}, and Fe^{3+}) ions. *Inorg. Chem.* **2021**, *60*, 1116-1123.

S4. Li, G. P.; Liu, G.; Li, Y. Z.; Hou, L.; Wang, Y. Y.; Zhu, Z. H. Uncommon pyrazoyl-carboxyl bifunctional ligand-based microporous lanthanide systems: sorption and luminescent sensing properties. *Inorg. Chem*. **2016**, *55*, 3952-3959.

S5. Zhang, Q. S.; Wang, J.; Kirillov, A. M.; Dou, W.; Xu, C.; Xu, C. L.; Yang, L. Z.; Fang, R.; Liu, W. S. Multifunctional Ln-MOF luminescent probe for efficient sensing of Fe^{3+}, Ce^{3+}, and acetone. *ACS. Appl. Mater. Interfaces* **2018**, *10*, 23976-23986.

S6. Sun, Z.; Yang, M.; Ma, Y.; Li, L. C. Multi-responsive luminescent sensors based on two-dimensional lanthanide-metal organic frameworks for highly selective and sensitive detection of Cr (III) and Cr (VI) ions and benzaldehyde. *Cryst. Growth Des*. **2017**, *17*, 4326-4335.

S7. Chen, M.; Xu, W. M.; Tian, J. Y.; Cui, H.; Zhang, J. X.; Liu, C. S.; Du, M. A terbium (III) lanthanide-organic framework as a platform for a recyclable multi-responsive luminescent sensor. *J. Mater. Chem. C* **2017**, *5*, 2015-2021.

S8. Zhang, X. L.; Zhan, Z. Y.; Liang, X. Y.; Chen, C.; Liu, X. L.; Jia, Y. J.; Hu, M. Lanthanide-MOFs constructed from mixed dicarboxylate ligands as selective multi-responsive luminescent sensors. *Dalton Trans*. **2018**, *47*, 3272-3282.

S9. Li, J. M.; Li, R.; Li, X. Construction of metal-organic frameworks (MOFs) and highly luminescent Eu (III)-MOF for the detection of inorganic ions and antibiotics in aqueous medium. *CrystEngComm* **2018**, *20*, 4962-4972.

S10. Zhang, X. J.; Su, F. Z.; Chen, D. M.; Peng, Y.; Guo, W. Y.; Liu, C. S.; Du, M. A water-stable Eu^{III}-based MOF as a dual-emission luminescent sensor for discriminative detection of nitroaromatic pollutants. *Dalton Trans.* **2019**, *48*, 1843-1849.

S11. Zhan, Z. Y.; Liang, X. Y.; Zhang, X. L.; Jia, Y. J.; Hu, M. A water-stable europium-MOF as a multifunctional luminescent sensor for some trivalent metal ions (Fe^{3+}, Cr^{3+}, Al^{3+}), PO_4^{3-} ions, and nitroaromatic explosives. *Dalton Trans*. **2019**, *48*, 1786-1794.

S12. Gogoi, C.; Reinsch, H.; Biswas, S. A pyrazine core-based luminescent Zr (iv) organic framework for specific sensing of Fe^{3+}, picric acid and $Cr_2O_7^{2-}$. *CrystEngComm* **2019**, *21*, 6252-6260.
S13. Duan, L. J.; Zhang, C. C.; Cen, P. P.; Jin, X. Y.; Liang, C.; Yang, J. H.; Liu, X. Y. Stable Ln-MOFs as multi-responsive photoluminescence sensors for the sensitive sensing of Fe^{3+}, $Cr_2O_7^{2-}$, and nitrofuran. *CrystEngComm* **2020**, *22*, 1695-1704.
S14. Liu, W.; Huang, X.; Xu, C.; Chen, C. Y.; Yang, L. Z.; Dou, W., Chen, W. M.; Yang, H.; Liu, W. S. A multi-responsive regenerable europium-organic framework luminescent sensor for Fe^{3+}, Cr^{VI} anions, and picric acid. *Chem. -Eur. J.* **2016**, *22*, 18769-18776.
S15. Du, Y.; Yang, H. Y.; Liu, R. J.; Shao, C. Y.; Yang, L. R. A multi-responsive chemosensor for highly sensitive and selective detection of Fe^{3+}, Cu^{2+}, $Cr_2O_7^{2-}$ and nitrobenzene based on a luminescent lanthanide metal-organic framework. *Dalton Trans.* **2020**, *49*, 13003-13016.
S16. Sun, Z.; Li, Y. G.; Ma, Y.; Li, L. C. Dual-functional recyclable luminescent sensors based on 2D lanthanide-based metal-organic frameworks for highly sensitive detection of Fe^{3+} and 2,4-dinitrophenol. *Dyes Pigments* **2017**, *146*, 263-271.
S17. Wang, Q. S.; Li, J. J.; Zhang, M. N.; Li, X. A luminescent Eu (III)-based metal-organic framework as a highly effective sensor for cation and anion detections. *Sensor Actuat. B-Chem.* **2018**, *258*, 358-364.